Facile Synthesis of Highly Luminescent Lithium Silicate Nanocrystals with Varying Crystal Structure and Morphology

*Ebtesam H. Eladgham,[1,2] Denis Demchenko,[3] Tanner A. Nakagawara,[4] Ümit Özgür,[4] and Indika U. Arachchige[1]**

[1]Department of Chemistry, Virginia Commonwealth University, Richmond, Virginia 23284, United States

[2]Department of Solar Energy, National Research Center, Dokki, Cairo 12622, Egypt

[3]Department of Physics, Virginia Commonwealth University, Richmond, Virginia 23284, United States

[4]Department of Electrical and Computer Engineering, Virginia Commonwealth University, Richmond, Virginia 23284, United States

Electronic Supplementary Information

*Email: iuarachchige@vcu.edu

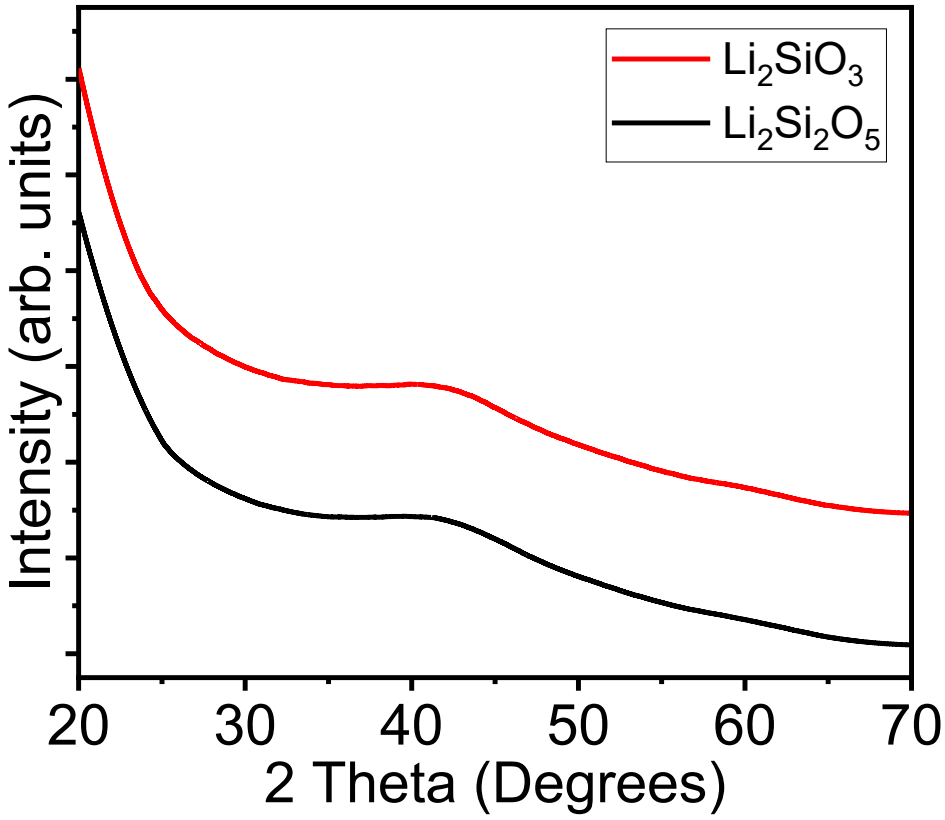

Figure S1. Powder X-ray diffraction pattern of amorphous-to-poorly crystalline $Li_2Si_xO_y$ NPs.

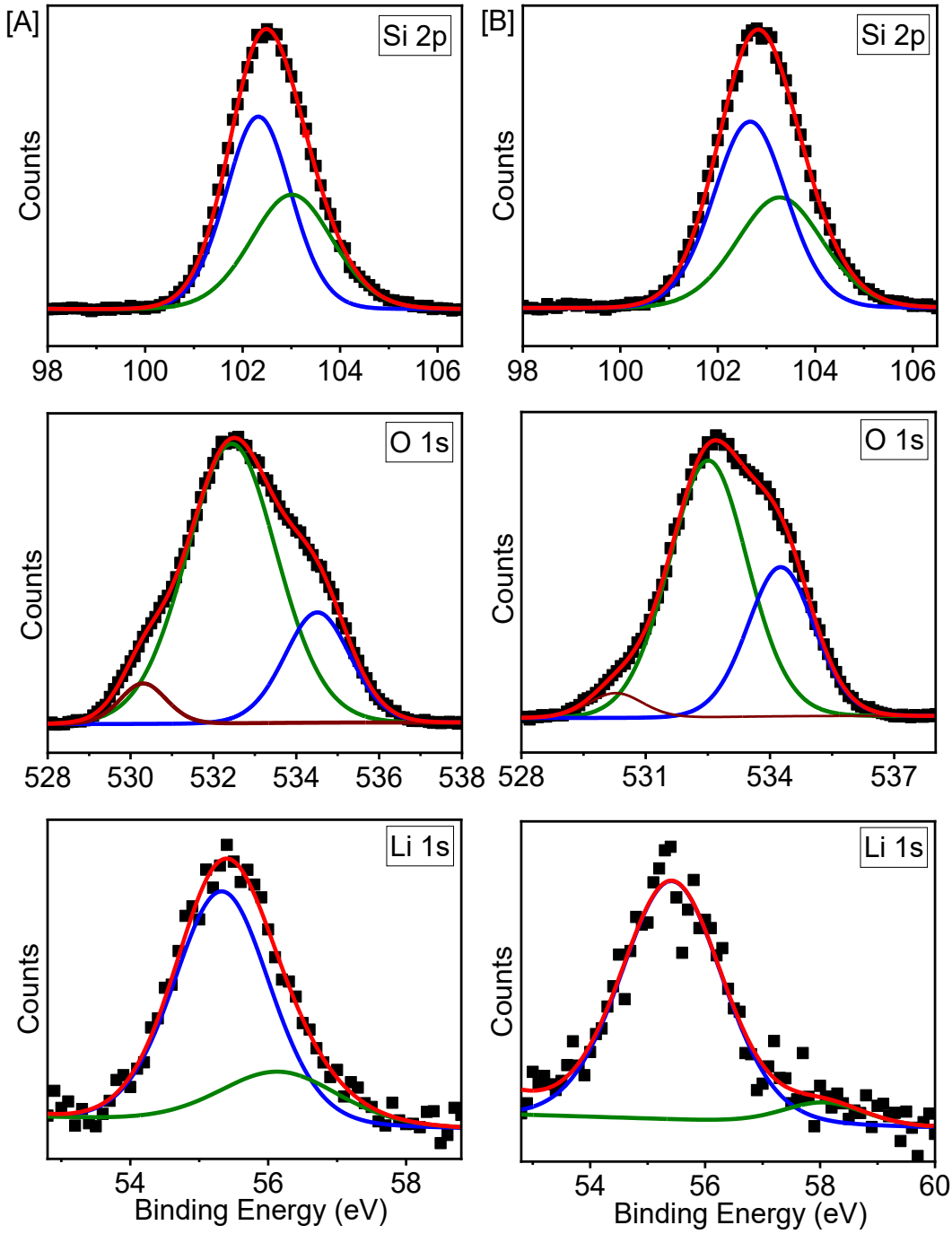

Figure S2. Si (2p), O (1s), and Li (1s) XPS spectra of as-synthesized, amorphous-to-poorly crystalline (A) Li_2SiO_3 and (B) $Li_2Si_2O_5$ NPs. Square symbols represent spectral data whereas the solid blue, green and wine lines are fitted deconvolutions. The red lines are spectral envelopes.

Table S1: Binding Energy Values Obtained from Si (2p), Li (1s), and O (1s) XPS spectra of amorphous-to-poorly crystalline Li_2SiO_3 and $Li_2Si_2O_5$ NPs.

Sample	Deconvoluted Peaks	Si 2p (eV)		Li 1s (eV)		O 1s (eV)		
		A	B	A	B	A	B	C
Li_2SiO_3		102.32	103.01	55.33	56.15	530.30	532.44	534.51
$Li_2Si_2O_5$		102.66	103.27	55.42	58.07	530.28	532.51	534.26

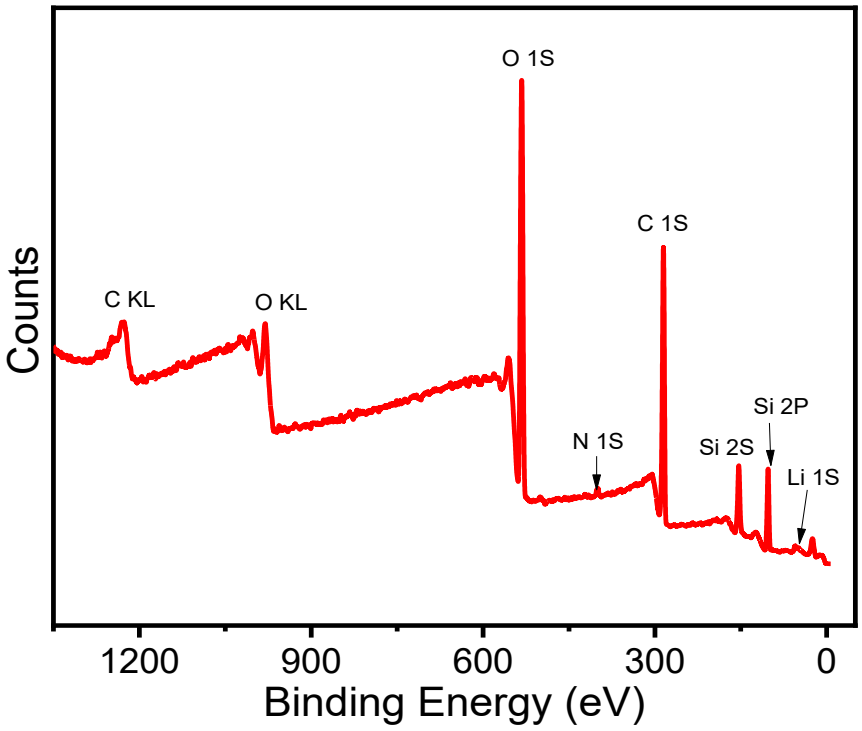

Figure S3. XPS survey scan of as-synthesized, amorphous-to-poorly crystalline Li_2SiO_3 NPs.

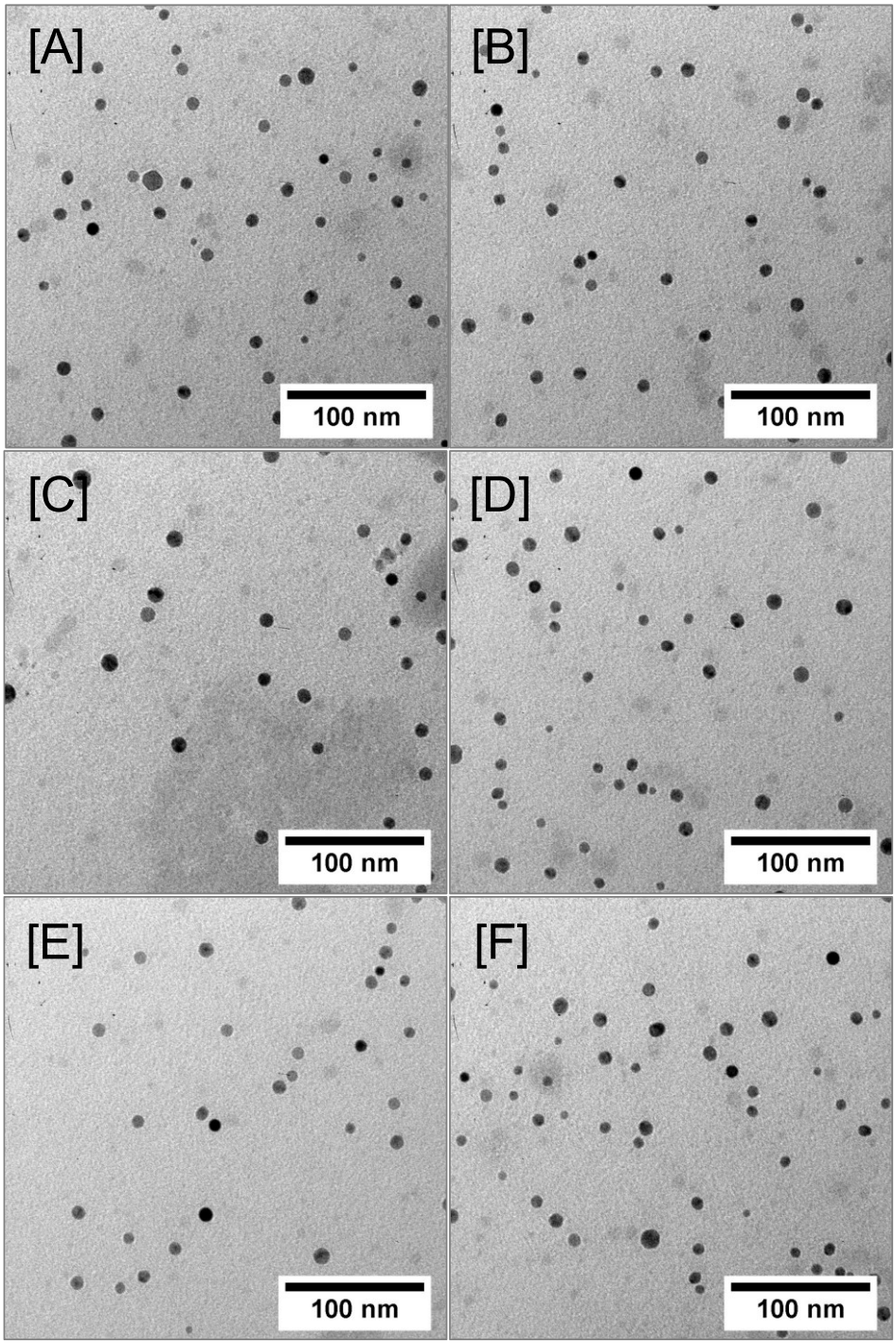

Figure S4. [A-F] Low resolution TEM images of amorphous-to-poorly crystalline Li_2SiO_3 NPs. Images A to F show different regions of the grid or distribution of NPs within the same sample.

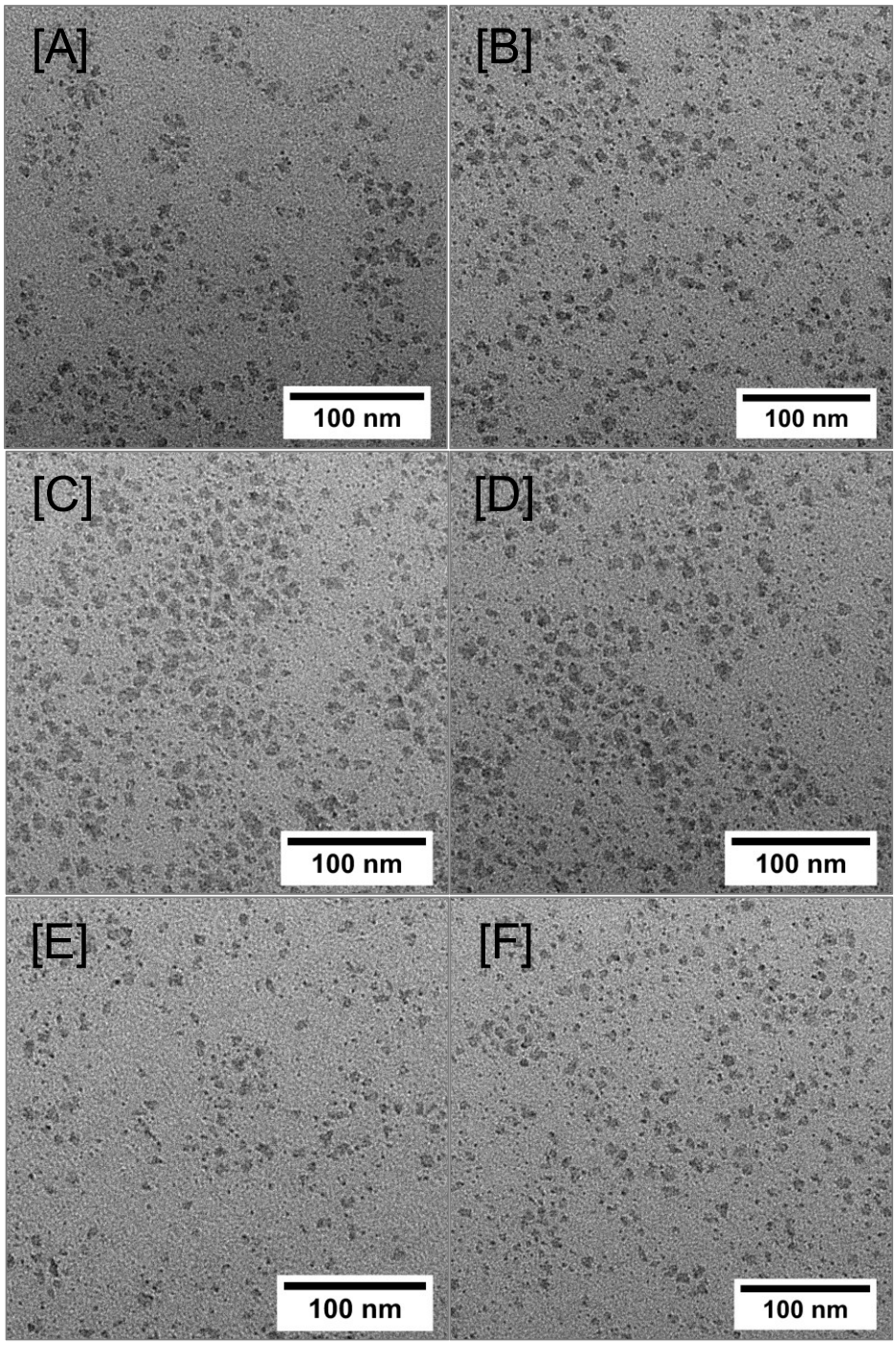

Figure S5. [A-F] Low resolution TEM images of amorphous-to-poorly crystalline $Li_2Si_2O_5$ NPs. Images A to F show different regions of the grid or distribution of NPs within the same sample.

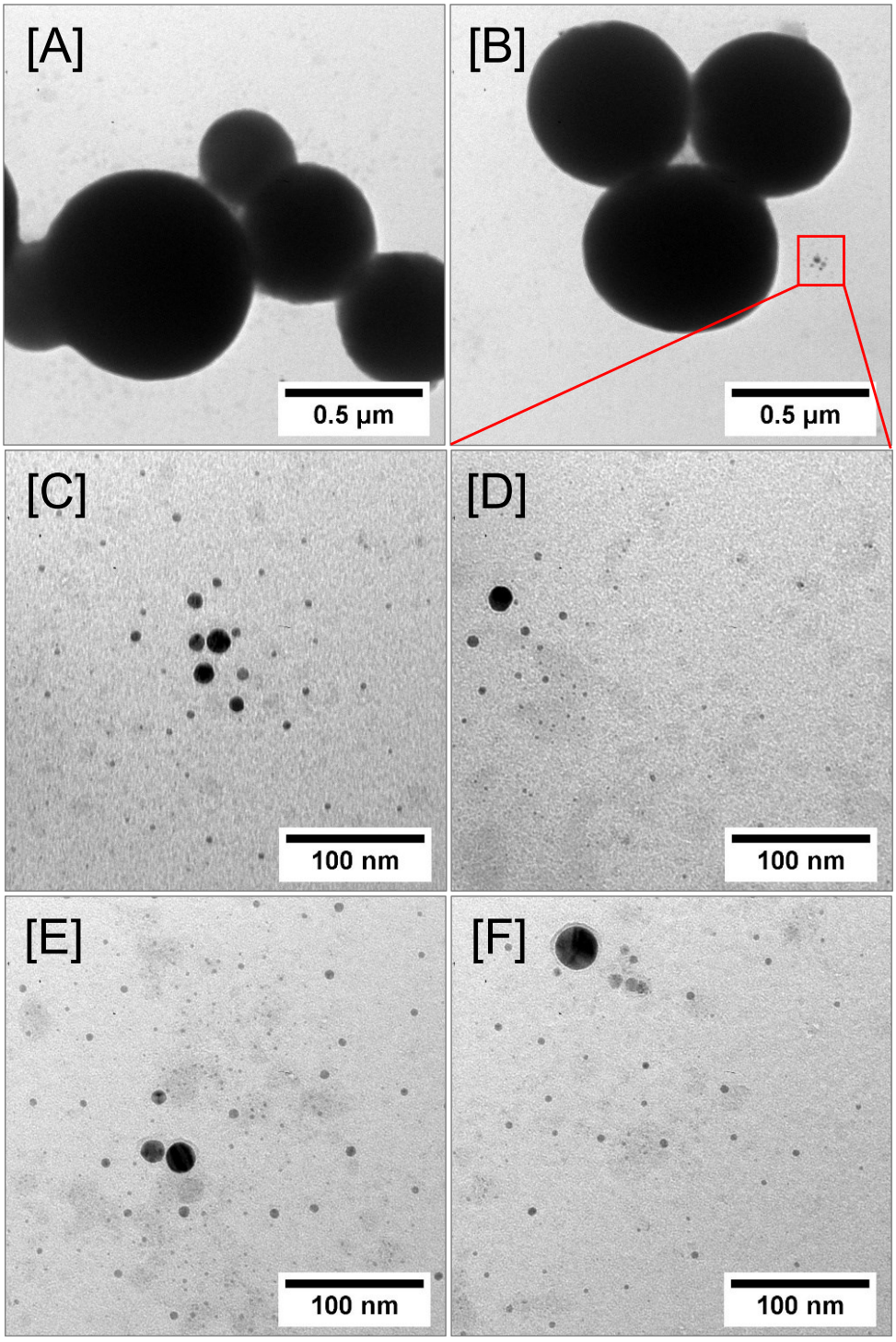

Figure S6. [A-F] Low resolution TEM images of phase-pure orthorhombic Li_2SiO_3 NPs produced via annealing of as-synthesized $Li_2Si_xO_y$ NPs at 600ºC for 2 h. Images A to F show different regions of the grid or overall distribution of NPs within the same sample.

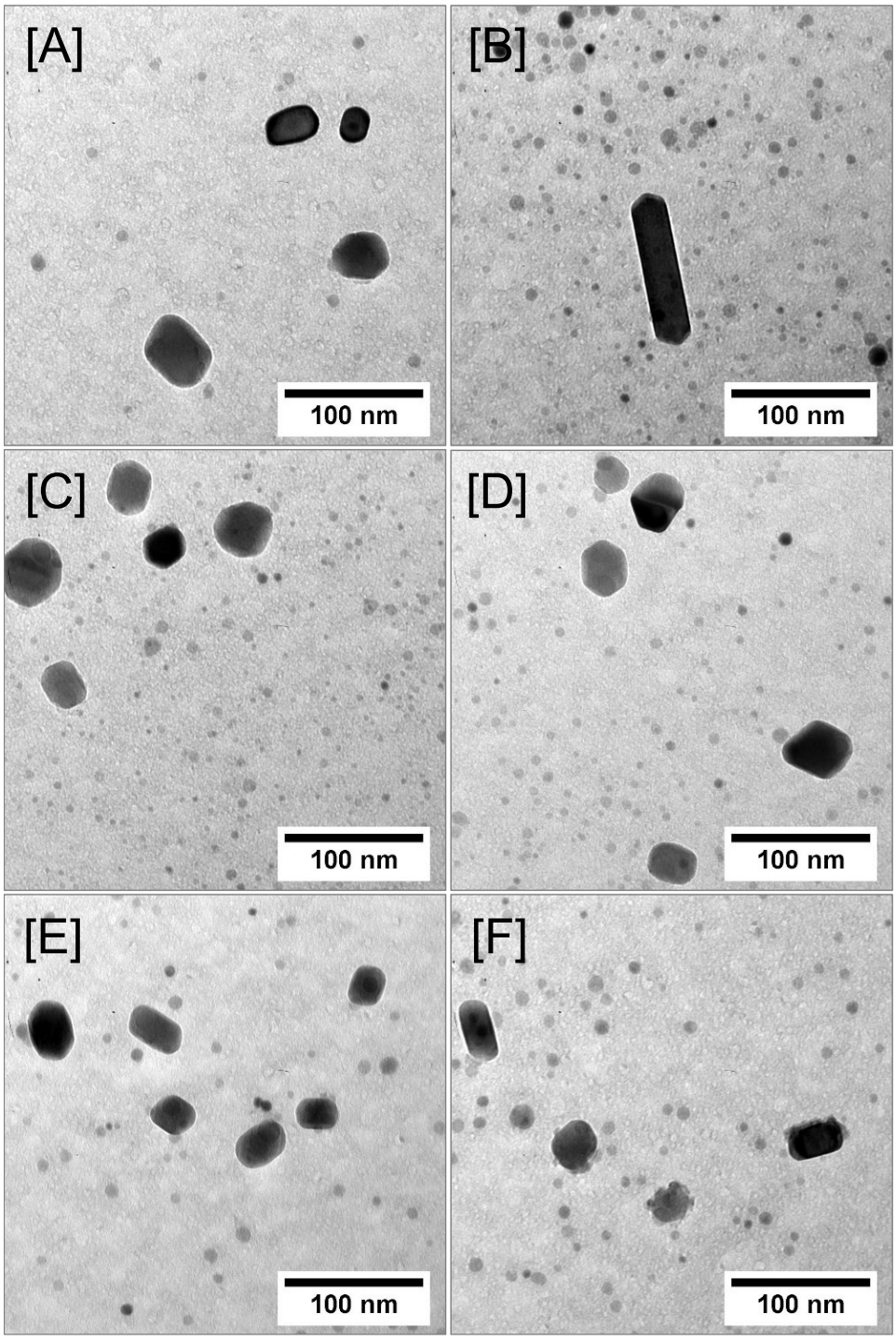

Figure S7. [A-F] Low resolution TEM images of phase-pure orthorhombic $Li_2Si_2O_5$ NPs produced via annealing of as-synthesized $Li_2Si_xO_y$ NPs at 600ºC for 2 h. Images A to F show different regions of the grid or overall distribution of NPs within the same sample.

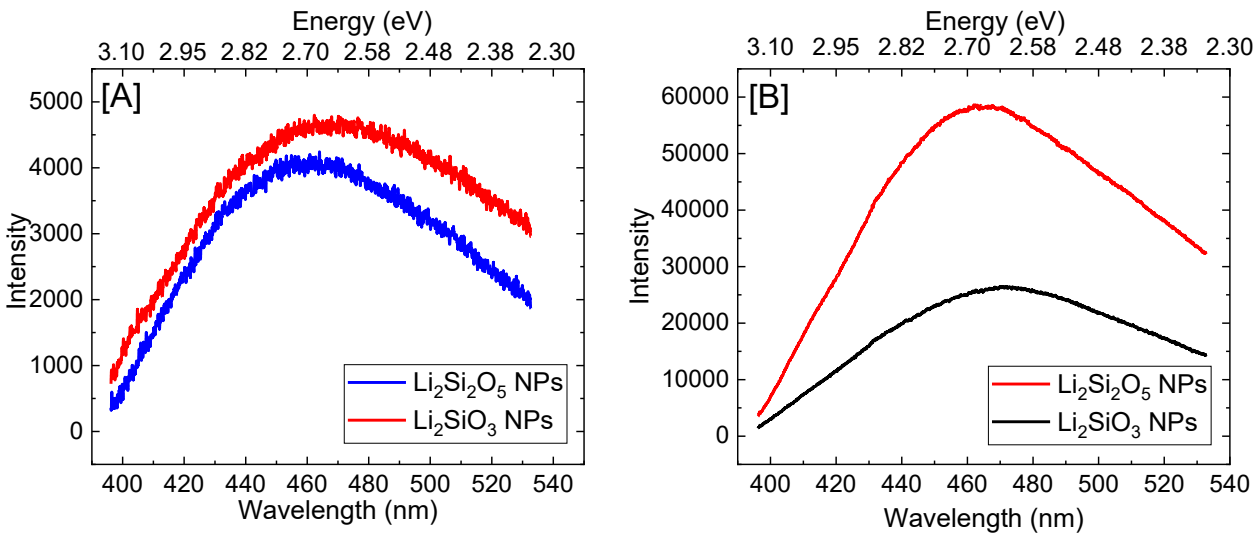

Figure S8. Solid state PL spectra of Li_2SiO_3 and $Li_2Si_2O_5$ NPs recorded at [A] room temperature (295 K) and [B] low temperature (15 K).

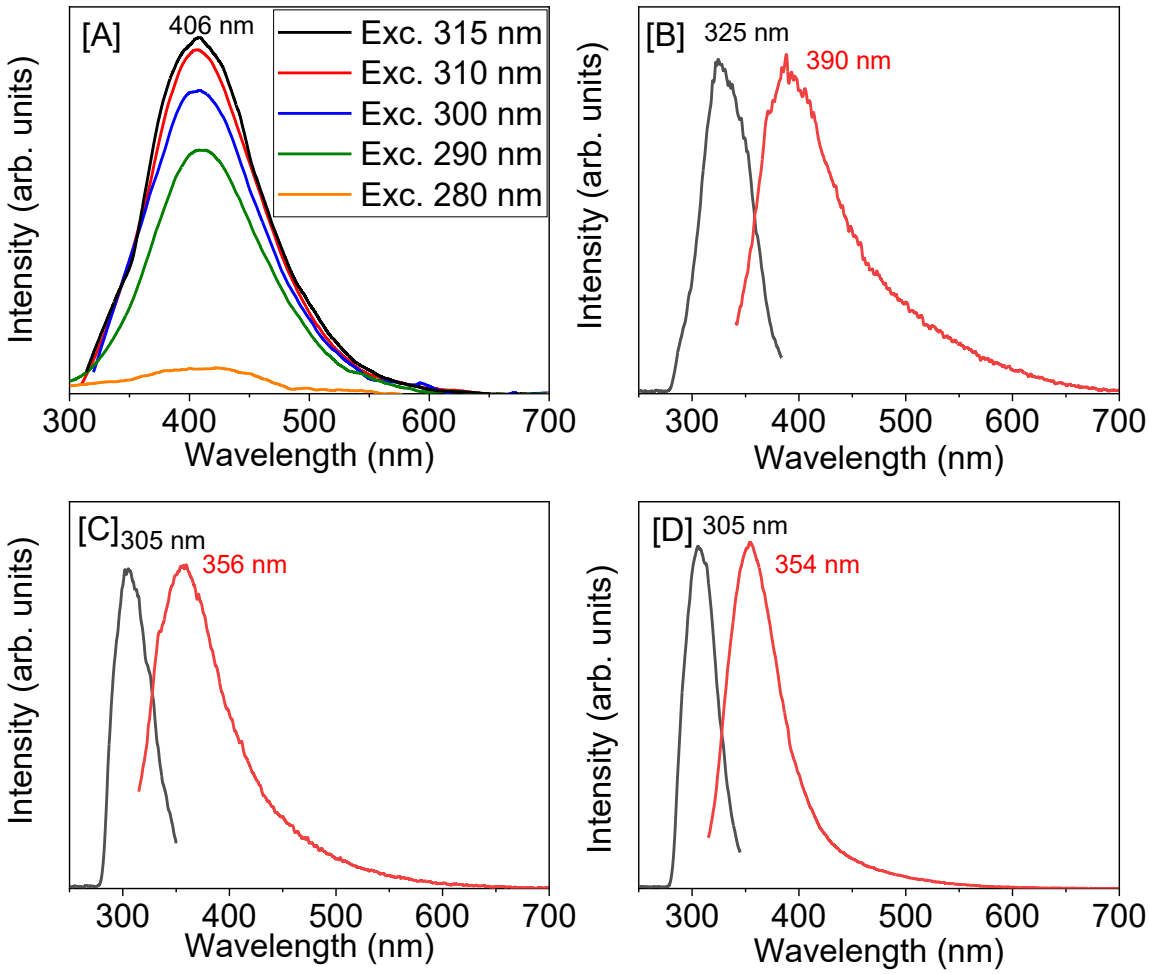

Figure S9. [A] Solution state PL spectra of as-synthesized $Li_2Si_xO_y$ NPs recorded at different excitation energies along with PL (red) and PLE (black) spectra of [B] OLA and HDD ligands at room temperature, [C] OLA and HDD ligands annealed at 250 °C for 30 min., and [D] OLA, HDD, and n-BuLi mixture annealed at 250 °C for 30 min. The spectra shown in B, C, D exhibit weak (QY = <1%), blue-shifted PL maxima than the high intensity (QY = 10-30%) visible PL observed in as-synthesized silicate nanocrystals.

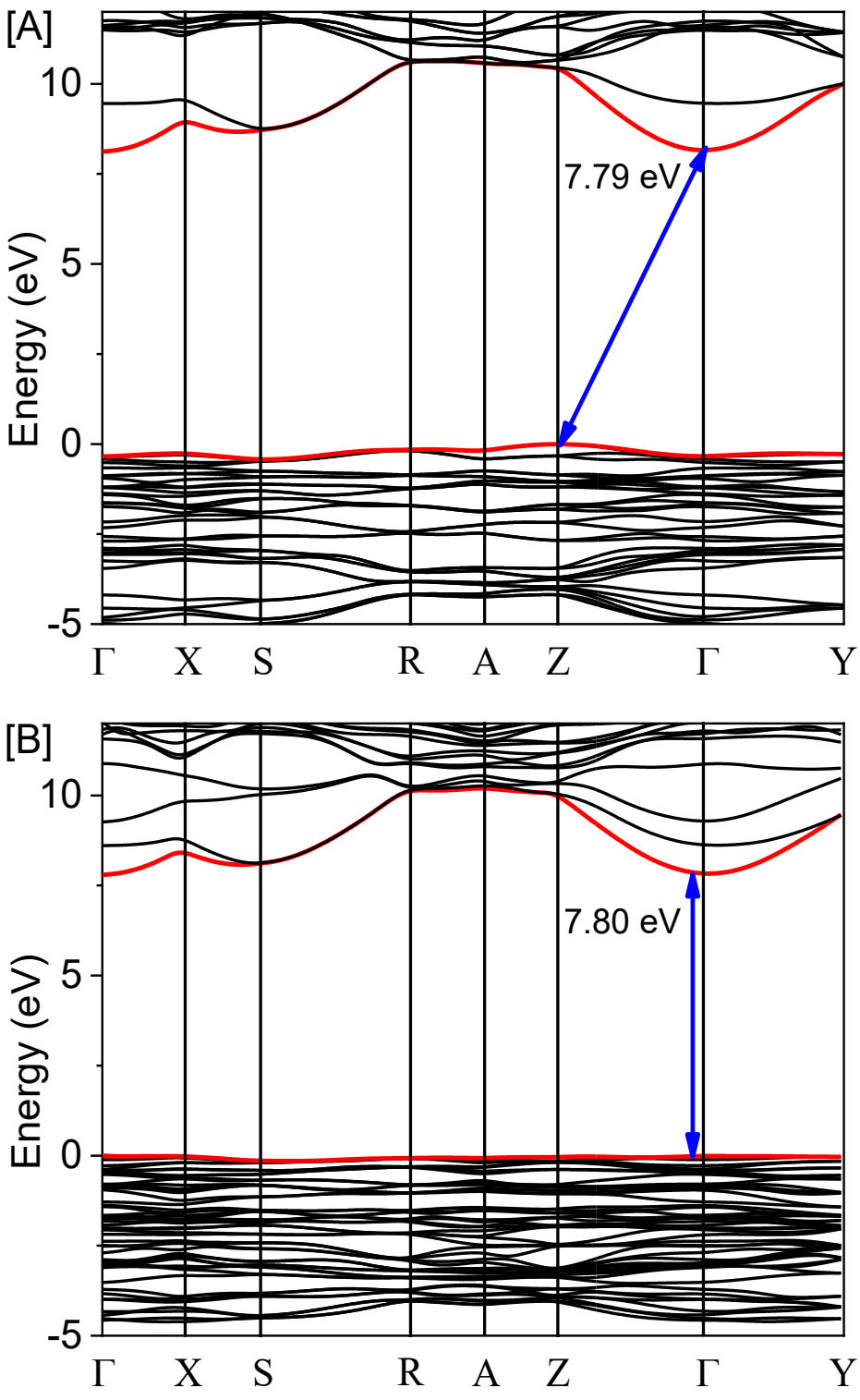

Figure S10. Band structures of (a) orthorhombic Li_2SiO_3 and (b) orthorhombic $Li_2Si_2O_5$ computed using HSE hybrid functional method.